8. The presence of triacylglycerols was confirmed by extracting lipids from both wild-type and pickle roots and separating the various lipids by thin-layer chromatography
9. J. B. Ohlrogge, J. Browse, C. R. Somerville, *Biochim. Biophys. Acta* **1082**, 1 (1991).
10. G. J. H. van Rooijen, L. I. Terning, M. M. Moloney, *Plant Mol. Biol.* **18**, 1177 (1992); J. H. E. Ross and D. J. Murphy, *Plant J.* **9**, 625 (1996).
11. E. Krebbers *et al.*, *Plant Physiol.* **87**, 859 (1988); P. Guerche *et al.*, *Plant Cell* **2**, 469 (1990).
12. K. Izumi, Y. Kamiya, A. Sakurai, H. Oshio, N. Takahashi, *Plant Cell Physiol.* **26**, 821 (1985).
13. T.-P. Sun and Y. Kamiya, *Plant Cell* **6**, 1509 (1994).
14. M. Koornneef, J. van Eden, C. J. Hanhart, A. M. M. de Jongh, *Genet. Res.* **41**, 57 (1983); T.-P. Sun, H. M. Goodman, F. M. Ausubel, *Plant Cell* **4**, 119 (1992).
15. M. Koornneef *et al*., *Physiol. Plant.* **65**, 33 (1985); J. Peng and N. P. Harberd, *Plant Cell* **5**, 351 (1993).
16. J. M. Fay, *Econ. Bot.* **45**, 16 (1991).
17. R. S. McClinton and Z. R. Sung, *Planta,* in press.
18. T. C. Verwoerd, B. M. M. Dekker, A. Hoekema, *Nucleic Acids Res.* **17**, 2362 (1989).
19. A. M. Metz, R. T. Timmer, K. S. Browning, *Gene* **120**, 313 (1992).
20. We thank C. Cassayre, S. Kaufmann, C. McNiff, K. Norton, D. Ogas, and A. Van for contributing to the project; P. Broun, D. Falcone, S. Reiser, F. Thomas, S. Ruzin from the NSF Center for Developmental Biology, and K. McDonald and P. Sicurello from the Electron Microscope Laboratory, University of California Berkeley for technical assistance; Y. Kamiya and Sumitomo Chemical Company Limited, Japan, for supplying uniconazole-P; *Arabidopsis* Biological Resource Center for supplying seed stocks; and S. Cutler, S. Gilmore, W. Lukowitz, S. Rhee, S. Turner, and J. Zeevaart for comments on the manuscript. Supported by grants to C.S. from the U.S. Department of Energy (DE-FG02-97ER20133) and to Z.R.S. from NSF (grant IBN-9513522). J.O. was supported by a postdoctoral fellowship from NSF.

25 February 1997; accepted 12 May 1997

Evolution of a Strain of CJD That Induces BSE-Like Plaques

Laura Manuelidis,* William Fritch, You-Gen Xi

Bovine spongiform encephalopathy (BSE) has become a public health issue because a recently evolved BSE agent has infected people, yielding an unusual form of Creutzfeld-Jakob disease (CJD). A new CJD agent that provokes similar amyloid plaques and cerebellar pathology was serially propagated. First-passage rats showed obvious clinical signs and activated microglia but had negligible PrP-res (the more protease-resistant form of host PrP) or cerebellar lesions. Microglia and astrocytes may participate in strain selection because the agent evolved, stabilized, and reproducibly provoked BSE-like disease in subsequent passages. Early vacuolar change involving activated microglia and astrocytes preceded significant PrP-res accumulation by more than 50 days. These studies reveal several inflammatory host reactions to an exogenous agent.

The recent epidemic of bovine spongiform encephalopathy (BSE) has brought increased attention to its human counterpart, Creutzfeldt-Jakob disease (CJD), as well as to scrapie, an endemic infection of sheep. Since the first recognized case of BSE in 1985, it is likely that more than one million cows have become infected by dietary exposure to scrapie-contaminated food (*1*). Domestic cats and various zoo animals have been similarly infected. Additional experimental propagation of the cow-derived agent in many species, including pigs, rodents, and primates (*2*, *3*), suggests that the new BSE agent has acquired an enhanced ability to evade host defenses. In 1996, the BSE agent was linked to a variant disease in younger people (*4*) that was reproduced in primates by BSE inoculation (*3*). Because human CJD infections can be undetectable for more than 20 years, it is likely that we will see more BSE-linked cases (*5*, *6*). Thus, there is an emerging public health issue that requires a greater understanding of agent strains and their specific interactions with the host.

Many different infectious strains of the scrapie and CJD agents have been propagated in inbred mice encoding the same PrP amino acid sequence (*7*, *8*). The main reasons why human "BSE" is considered to be caused by a new agent strain are based on (i) the youth of most victims (less than 30 years old), (ii) the prolonged clinical course, (iii) severe involvement of the cerebellum, and (iv) the presence of many large plaques. Sporadic CJD, which accounts for ~90% of CJD worldwide and is infectious in a variety of species (*9*, *10*), rarely shows cerebellar pathology or widespread plaques. Only two other human transmissible encephalopathies with a long clinical phase display cerebellar lesions and a plaque-rich phenotype. These are kuru, an infection transmitted by ritual cannibalism (*9*), and Gerstmann-Straussler-Sheinker disease (GSS), a group of rare "familial" forms of CJD (*11*).

One explanation for these different phenotypes focuses on mutations in host PrP. It has been suggested that a combination of mutations causes PrP to fold into an infectious conformation that encrypts and propagates strain-specific information (*12*). However, people infected with "BSE" do not have any of the plaque-associated PrP mutations such as Phe^{102} to Leu^{102} (*13*). Alternatively, a newly mutated exogenous virus may provoke unusual phenotypic responses in the host, including different forms of PrP-res (*8*). Additional host responses could signify recognition of the foreign agent hidden within cells. Because strong lymphocyte responses are evaded, it is often stated that these infections lack any inflammatory component (*9*, *14*). We found that inflammatory cells can participate in the evolution of a new infectious strain. This strain causes a disease with notable similarity to both "familial" GSS and human "BSE" and evokes inflammatory reactions at early stages of infection.

To change an established CJD strain into one that could produce plaques and cerebellar lesions, we inoculated alternate species without manipulating normal host PrP sequences. Unusual inflammatory responses in microglia or astrocytes (or both) were used to evaluate host recognition. Such responses could subject the agent to more rigorous selective pressures favoring a mutated plaque-evoking strain. We therefore challenged several types of inbred mice, Chinese hamsters, and rats with a strain of CJD (designated SY) that was highly selected by serial passage 5 times in guinea pigs and then 24 times in Syrian hamsters (*15*). SY was successfully transmitted to all three species and had a relatively prolonged incubation period even after serial passage (>350 days). Only the rats showed remarkable pathology.

In the first passage (P1), only two of six rats (killed at 672 and 732 days) showed obvious spongiform changes (*16*). The 672-day rat exhibited clear clinical signs (startle myoclonus in response to noise, hunched posture, and terminal lack of feeding and grooming). The progression to terminal disease was rapid, lasting only 8 days. The 732-day rat showed no clinical signs, but both animals had a similar distribution of vacuoles and these were located predominantly in the cerebral cortex and to a lesser extent in CA1 and CA2 of the hippocampus. Only nonspecific aging changes were seen in the cerebellum. PrP-res was not detected in histological sections from the clinically ill rat, although very rare PrP deposits were found near the inoculation site in the nonclinical rat. The most unusual finding in both rats was a marked increase in reactive microglia in the cerebrum, even in regions with minimal vacu-

Section of Neuropathology, Yale Medical School, 310 Cedar Street, New Haven, CT 06510, USA.

*To whom correspondence should be addressed. E-mail: laura.manuelidis@yale.edu

olization (Fig. 1A). In contrast, the same region of the cortex from a P1 rat scored as negative for CJD showed few keratan sulfate (KS)–positive microglia at 592 days (Fig. 1B), as did uninoculated control rats (*17*). Staining of astroglial filaments with antibodies to glial fibrillary acidic protein (GFAP) showed a pathological increase in hypertrophic astrocytes, a universal characteristic of CJD infections (*10, 15, 18*).

A portion of the 672-day rat brain was used for the second passage, because the marked vacuolization without PrP-res indicated replication of an unusual infectious strain. There was a dramatic decrease in incubation period in P2, yielding a mean of 477 ± 18 days (SEM), and all rats showed clinical signs (n = 7). The reduction in incubation time, combined with the 100% mortality, indicated that the infectious agent had become more virulent for its new host (*19*). More widespread and severe spongiform changes further confirmed an enhanced virulence in P2. Other features were more unusual. Most remarkable was the vacuolization of many GFAP+ astrocytes around the lateral ventrical and in the thalamus (Fig. 1C). Fulminant astrocytic vacuolization signified further strain selection and has not been seen in other transmissible encephalopathies. There was also a change in the distribution of lesions during P2. The cerebellum had many vacuoles, especially in the internal granule cell layer, and Ammon's horn was now involved. Severe cerebellar lesions that occur in kuru, "familial" GSS and human "BSE" have not previously been seen in nonprimate infections. Additionally, several mature plaques with a halo of radial fibers were observed in Ammon's horn. These, as well as less obvious plaques in the cerebral cortex, had a central core of PrP (Fig. 1D). Plaques were larger than neurons and typically measured ≥20 μm in diameter. Ultrastructurally, they had characteristic extracellular amyloid fibers (Fig. 1E). These widespread plaques are entirely different from the small PrP deposits (1 to 4 μm) associated with severe vacuolization in other passaged CJD isolates (*12*). Finally, PrP often surrounded capillaries and other thin-walled vessels (Fig. 1F), which suggested abrogation of the blood-brain barrier. An increase in astrocytes and reactive microglia around these vessels, as well as elsewhere in the parenchyma, was consistent with an inflammatory or reactive process. These cells may be involved in recognition and selection of the infectious agent.

We stabilized this new strain by serial passage. In P3, there was a small additional decrease in incubation time (441 ± 10 days; n = 10). However, the length of time from appearance of clinical signs to terminal disease was increased in P3 (>45 days) as compared with an interval of <26 days in P2 rats. This represents a rat equivalent of chronic CJD or GSS in terms of a rat lifetime and signifies further agent evolution. In P3 and P4, clinical signs of cerebellar dysfunction also became more prominent (*20*). Despite an incremental reduction in incubation time (to ~350 days by P4), the plaques and cerebellar changes described above were perpetuated and were more pronounced, and end-stage birefringent plaques became more abundant in the cerebellum. The marked vacuolization of astrocytes was not propagated in P3 and P4, possibly indicating that the infectious agent was now escaping some host surveillence mechanisms.

With the single exception of a mouse scrapie strain, no other strains of scrapie or CJD have resulted in a true plaque-producing infection that can be propagated (*12, 21*). Plaques in P3 and P4 showed strong "Maltese cross" birefringence comparable to that seen in "familial" GSS (Fig. 2, A through C). These amyloid properties cannot be explained on the basis of the host PrP sequences because these are known to be discordant in rat and human (*22*). Additionally, SY passaged in inbred mice with an equivalent 350- to 550-day incubation period (*8*) showed no plaques despite the known concordance of mouse and rat PrP in amyloid folded regions (*22*). Thus, these two SY strains produce disease variants that are unrelated to primate PrP sequences or incubation time.

Microglia are cellular chameleons. They act as Trojan horses carrying infectious agents into the brain and can participate in lytic responses and antigen presentation. We therefore evaluated a human "BSE" sample using the more available and specific antibodies for human leukocyte class II antigens (HLA-DR). Positive staining was seen in plaques and other regions (Fig. 2D) that was comparable to the pattern of microglial infiltration in rat CJD (Fig. 2E). Additionally, astrocytic responses were similarly florid in both the human and rat specimens (Fig. 2, F

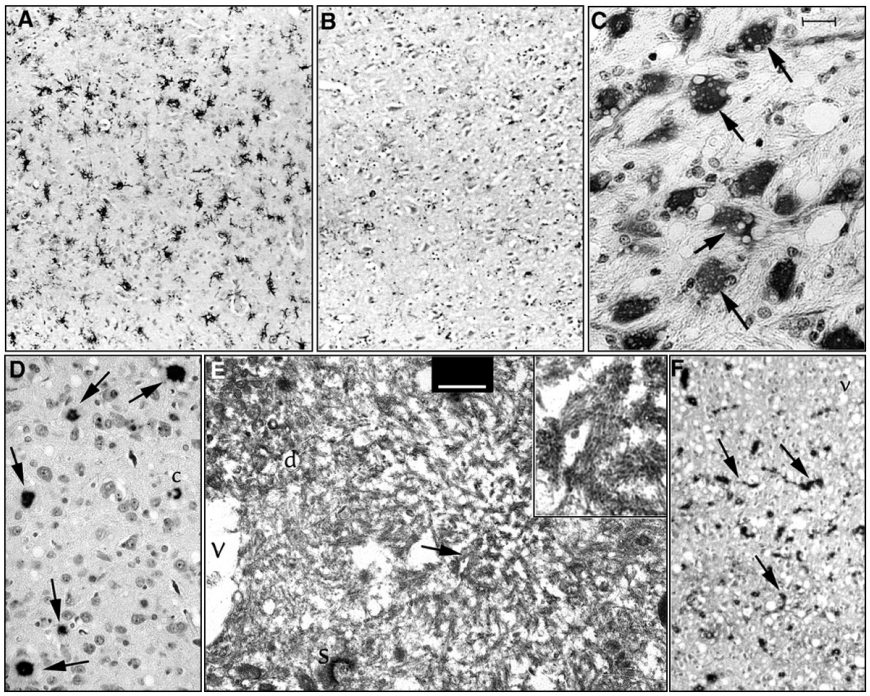


Fig. 1. Pathology in P1 and P2 rats; the tissue was not autoclaved (*18*). (**A**) P1-positive rat at 672 days used for transmission. Many KS+-reactive microglia (black cells) are obvious even in the cortical region without many vacuoles (see Fig. 2E for typical higher magnification morphology). (**B**) The same region from the P1 (CJD-negative) rat at 592 days, showing few KS+ cells (parallel staining, same magnification). (**C**) P2 rat at 512 days with remarkable vacuolization in reactive GFAP+ astrocytes (arrows) in the region adjacent to the lateral ventricle. Other GFAP+ astrocytes were more stellate (see Fig. 2G). Scale bar, 10 μm. (**D**) PrP-decorated plaques in P2 (arrows). The immunostained inner dark cores of the mature plaques (corner arrows) measured ≥10 μm, and with the pale radial periphery were ≥20 μm in diameter. A PrP-positive capillary (c) and some vacuoles are present in this cortical region. (**E**) Electron micrograph of the edge of a cerebellar plaque bordered by a degenerating neurite (d), a vacuole (v), and a preserved synapse (s). The inset shows higher magnification of dense radial and fibrillar amyloid fibrils from the region at the arrow. Microglia and hypertrophic astrocytes were identified adjacent to plaques. (**F**) Capillaries and small vessels with deposits of PrP (arrows) in a cerebral region with severe vacuolar change in P2.

and G). The abnormal blush of astrocytic processes around thin-walled vessels in human "BSE" (Fig. 2D, arrow) and the numerous migrating microglia around thin-walled vessels in infected rats could indicate breakdown of the blood-brain barrier in both instances.

To understand the sequential contribution of microglia, astrocytes, and molecular components in pathogenesis, we evaluated brains of P4 rats at 50-day intervals after inoculation. Uninoculated half-brains were used for histological studies to exclude pathological change caused by the inoculum. The other halves of these brains were pooled for independent quantitative RNA and protein blot studies (*23*). We assumed that vacuolar change would occur only late in infection. This is the classic sequence in SY-infected hamsters, in which high infectious titers provoke a sudden accumulation of PrP-res, which is then followed by vacuolization and clinical illness (*15*). Instead, vacuolization was the first indicator of infection, and major PrP deposition occurred 100 days later. At 100 days after inoculation, only a few vacuoles were observed, as representatively shown in the cerebellum in Fig. 3A. By 150 days, vacuolization was apparent in the cerebellum, hippocampus (Fig. 3, B and C), thalamus, and cortex. By 200 days, vacuolization was more severe and was very widespread. In addition to involvement of the hippocampus and cerebellum (now including the molecular layer), many regions had ballooned neuronal processes as shown in the thalamus (Fig. 3D). Figure 3E shows a graphic representation of these results when scored on a scale of 0 to 4. An early increase in activated microglia (KS-positive) closely paralleled the vacuolar progression, and focal regions of the cortex showed a clear increase by 150 days (*24*). In contrast, only extremely rare and tiny deposits of PrP were found at 150 days, and by 200 days these tiny deposits were three to four times more numerous in only a few brain regions. No PrP deposits of >4 μm could be found. Thus, these minor PrP accumulations were insufficient to explain the very widespread and profound vacuolization seen at 200 days.

Because ubiquitin acts as a chaperone for misfolded proteins, it can denote changes in PrP as well as other cellular proteins. Apolipoprotein J (ApoJ) can indicate inflammation-associated complement and membrane-attack complexes in other neurodegenerative diseases (*25*). Additionally, β-amyloid precursor–like proteins (APLP), thought to stabilize plaques in Alzheimer's disease (*26*), were used to indicate late-stage extracellular plaque formation. All these components, as well as ApoE, were strongly positive in plaques (*23, 27*).

There were low levels of ubiquitin at 150 and 200 days, comparable to levels of PrP-res. At 250 days, however, the ubiquitin response was far more pronounced than the PrP change. Ubiquitin accumulates in many neurodegenerative diseases. In contrast, ApoJ and APLP appeared late in disease and had the same profile as PrP deposition (Fig. 3E). The late change in ApoJ signified a final inflammatory response in the brain associated with plaque formation or possibly high agent titers. However, study of the spleen indicated an earlier response to the exogenous agent. At day 100, ApoJ cells were seen only at the center of the white pulp, whereas peripheral resident macrophages were rarely labeled. There was a dramatic increase in the number of ApoJ resident macrophages at 150 days (*27*); and, remarkably, a number of these macrophages showed vacuoles similar to those found in P2 astrocytes (see Fig. 1C). At 200 days and after, ApoJ-positive macrophages were equally abundant in the spleen, but vacuolization was reduced. This indicated an early systemic response to infection that coincided with early brain vacuolization. The vacuoles in resident spleen macrophages could

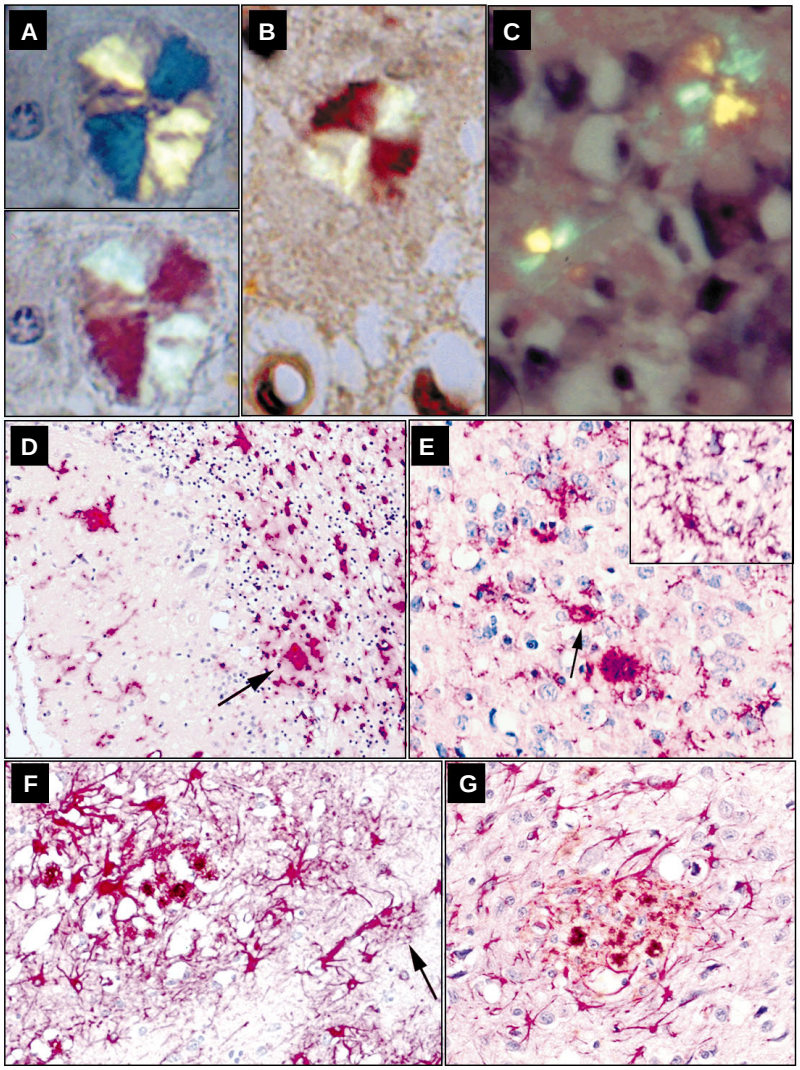


Fig. 2. (**A** through **C**) Congo Red birefringence. For reference, (A) shows a "Maltese cross" in an antibody-verified β-amyloid plaque at 0° (top; crossed polarizers) and at +9° (bottom), with the use of a 1/30 λ plate. Note the shift from green to red at +9°. The astrocyte nucleus at left is for size reference (5 to 6 m in diameter). (**B**) Similar Maltese cross positive PrP plaque adjacent to vacuoles in transmissible "familial" GSS (Leu^{102}). (C) Maltese cross positive rat plaques that had the same λ plate shifts. (**D**) HLA-DR (red) in human "BSE" cerebellum with infiltration of plaque at arrow. (**E**) KS+ microglia (red) and PrP-res (brown) show a similar picture of microglial infiltration. Numerous KS processes surround a PrP plaque in the hippocampus and a reactive microglial cell contains a deposit of PrP-res (arrow). The inset shows numerous processes of activated microglia in the cortex. (**F** and **G**) Double-staining for GFAP (red) and PrP-res (brown) with hematoxylin counterstain for nuclei (blue). (F) shows human "BSE." Hypertrophic astrocytes and extensive astrocytic processes surround PrP accumulations as well as a cortical vessel (arrow). (G) shows similar stellate astrocytes around a developing plaque in rat CJD.

signify viral clearance or destruction. These macrophages did not contain PrP-res.

To further exclude observer bias in the scoring of PrP, independent quantitative molecular experiments were then performed (*23*). PrP-res increases duplicated those found by histological scoring. Most PrP-res accumulated at 250 days and thereafter (Fig. 3F, left). At 300 days, PrP-res accounted for ~70% of the total PrP in the brain, as determined by densitometry of undigested and digested homogenates. Thus, almost all host PrP was suddenly altered at a later stage of disease. In contrast, when vacuolization was obvious at 150 days, PrP-res accounted for <1% of that found at 300 days. This PrP-res value is less than the value determined by histological assessment, even though cerebellar slices with early vacuolar change were overrepresented in the protein samples (*23*). It may be argued that at 150 days, low levels of PrP-res were sufficient to induce the more abundant vacuolization. However, this seems unlikely because PrP-res levels that are 10 times higher have failed to induce vacuoles in other CJD-infected rodents (*15*). The most straightforward explanation is that the new infectious agent induced significant vacuolization by non-PrP pathways. Moreover, the clinically ill rat from P1 (with widespread spongiform change) failed to show detectable PrP-res in highly sensitive assays (*23*). Thus, PrP-res again was not necessary for vacuolar change nor for clinical symptoms.

Astrocytic activation also coincided with vacuolization in a more convincing way than PrP-res. Figure 3F (right) shows a representative RNA blot from the same animals used for histological study. The profile of hybridization to the GFAP probe was compared with hybridization with a glyceraldehyde-dehydrogenase (GAD) probe. The latter probe, as well as other markers, confirmed that lanes had equivalent loads of RNA. There was a fivefold increase in GFAP mRNA between 100 and 150 days, and GFAP mRNA continued to increase with time. The above studies implicate both astrocytes and activated microglia in the early vacuolization induced by this infectious strain, possibly through neurotoxic and inflammatory cytokines.

The present studies show that an established agent can evolve in response to host defenses and become capable of provoking a rare constellation of GSS- and BSE-like lesions. Both the species barrier and the host responses to these foreign agents are more complex than predicted by the host's PrP sequence. Although small differences in glycosylation of one PrP-res band have been found in human "BSE" (*28*), deglycosylation of PrP has no effect on infectious titer or pathology in experimental CJD (*29*). The ability of these agents to change and to provoke different responses in the same host has public health implications. Strains that are present in the food chain and other products (*5, 6*) can evolve to cause variable host responses. Thus, public health officials might consider more than plaque-positive phenotypes in surveys for human "BSE" infections. Early diagnosis is also essential for rational exclusion of infected animals and medical products. Because CJD and BSE can be transmitted from samples without detectable PrP-res (*15, 30*), other markers for early infection are needed. Systematic molecular dissections have indicated that an ~27-nm particle with a viral-like density is infectious (*31*), and infectivity is recovered only when these nucleic acid–capsid particles remain intact (*32*). Thus, it seems reasonable to pursue cDNAs strategies in settings where candidate viral sequences can be defined (*8, 33*).

Early inflammatory responses may also be helpful. Although all recombinant or transgenic forms of PrP have failed to show significant infectivity (*34*), changes in host PrP can be part of a self-destructive cascade (*15, 35*), and host PrP is clearly

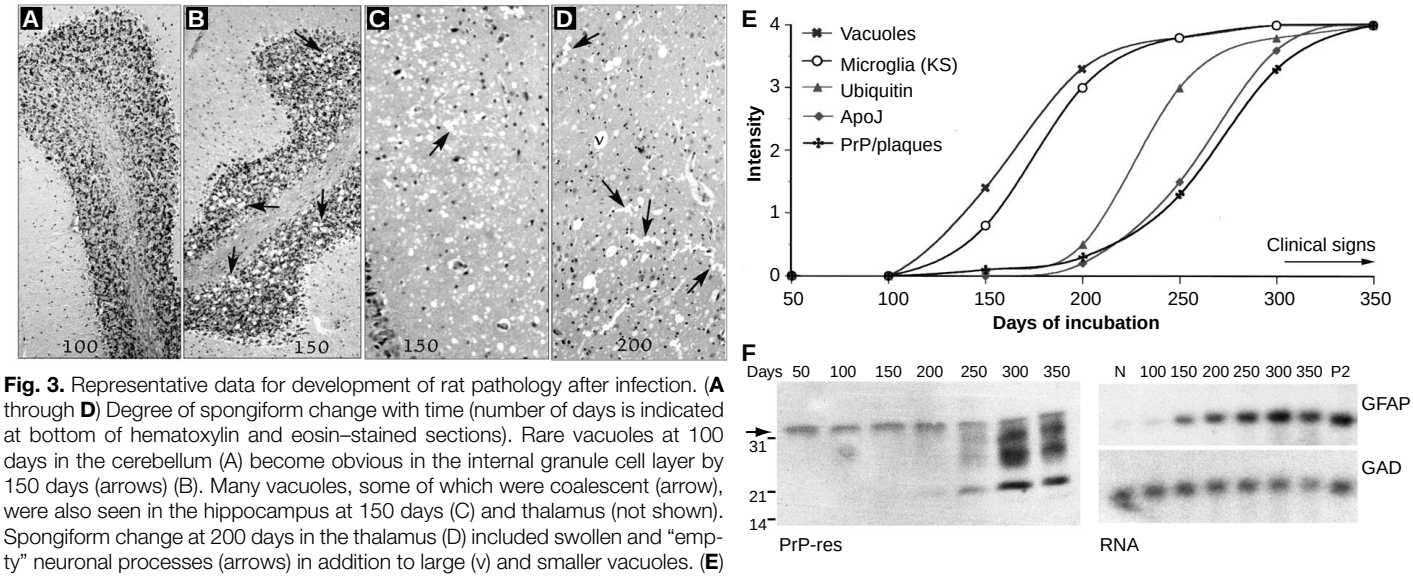


Fig. 3. Representative data for development of rat pathology after infection. (**A** through **D**) Degree of spongiform change with time (number of days is indicated at bottom of hematoxylin and eosin–stained sections). Rare vacuoles at 100 days in the cerebellum (A) become obvious in the internal granule cell layer by 150 days (arrows) (B). Many vacuoles, some of which were coalescent (arrow), were also seen in the hippocampus at 150 days (C) and thalamus (not shown). Spongiform change at 200 days in the thalamus (D) included swollen and "empty" neuronal processes (arrows) in addition to large (v) and smaller vacuoles. (**E**) Graph of pathological changes in P4 at 50-day intervals after inoculation (scored on a relative intensity scale of 0 to 4, as an average of two brains in multiple representative coronal sections where 0 is no change from normal, 1 = 1/4 maximal change, 2 = 1/2 maximal change, 3 = 3/4 maximal change, and 4 = maximal terminal change). Each feature, in relative order of appearance, shows the relative intensity at each time point. Tiny rare deposits of PrP-res are indicated by a score of <0.5 at 150 and 200 days, whereas more widespread deposits or plaques (or both) are indicated by later higher scores. The sequential appearance of markers and the relative severity of the changes were confirmed by a second blinded observer. Clinical signs started after 300 days (arrow). (**F**) Protein (left) and RNA (right) blots at indicated times. In the protein blot, equal loading is indicated by higher molecular weight protein (arrow). The lower three PrP-res bands (of ~29, 26, and 21 kD) became prominent only at 250 days after inoculation, and there was no residual PrP in the slots (not shown). Other blots with maximal loads and overexposure times failed to detect any PrP-res in the clinically ill P1 rat used for transmission (*23*). The Northern blot of total RNA on the right shows an earlier and more abundant increase in GFAP mRNA as compared with PrP-res at 150 days. For reference, the same Northern blot hybridized to a control GAD probe shows equivalent loads in each lane, as did the ethidium-stained gel used for blotting (not shown). N is total RNA from an uninoculated rat, and P2 shows the same final change in an earlier passage. The size of the GFAP mRNA band was ~2.7 kb and that of the GAD band was ~1.4 kb, which are close to their previously determined values (*15*).

involved in susceptibility to infection (*36*). Indeed, we suspect that the involvement of PrP in these diseases may derive from a natural role in inflammation. Nevertheless, the present studies indicate additional early inflammatory pathways in which astroglia, microglia, and even spleen macrophages recognize or incorporate the invading agent. Early vacuolated spleen macrophages can signify a peripheral site where the agent fights for its survival, and infected macrophages may eventually penetrate the blood-brain barrier in the natural disease. It is therefore pertinent to pursue chemical treatments that interfere with macrophage function because these can abolish early infections (*37*) and perhaps limit transient bursts of viremia (*38*). The recent observations of T lymphocytes in the brain at early stages of scrapie, susceptibility changes in mice with severe combined immunodeficiency disease, and the HIV-like paradoxical response to immunostimulatory and immunosuppressive compounds (*39*) further emphasize an important role for inflammatory and immune cells in strain-specified infections.

REFERENCES AND NOTES

1. R. Anderson *et al*., *Nature* **382**, 779 (1996).
2. M. Dawson, G. Wells, B. Parker, A. Scott, *Vet. Rec.* **127**, 338 (1990); M. Bruce *et al*., *Philos. Trans. R. Soc. London Ser. B* **343**, 405 (1994).
3. C. Lasemézas *et al*., *Nature* **381**, 733 (1996); A. Aguzzi, *ibid.*, p. 734.
4. R. Will *et al*., *Lancet* **347**, 921 (1996).
5. L. Manuelidis, *Transfusion* **34**, 915 (1994).
6. ———, *J. NeuroVirol.* **3**, 62 (1997).
7. I. Pattison and G. Millson, *J. Comp. Pathol.* **75**, 147 (1961); I. Pattison, *Res. Vet. Sci.* **7**, 207 (1966); M. E. Bruce and A. G. Dickinson, *J. Gen. Virol.* **68**, 79 (1987).
8. L. Manuelidis, in *Transmisssible Subacute Spongiform Encephalopathies: Prion Diseases*, L. Court and B. Dodet, Eds. (Elsevier, Paris, 1996), pp. 375–387.
9. D. C. Gajdusek, *Science* **197**, 943 (1977).
10. E. E. Manuelidis, *ibid.* **190**, 571 (1975); E. E. Manuelidis, E. J. Gorgacz, L. Manuelidis, *Nature* **271**, 778 (1978); *Proc. Natl. Acad. Sci. U.S.A.* **75**, 3432 (1978); J. Tateishi, T. Kitamoto, M. Hoque, H. Furukawa, *Neurology* **46**, 532 (1996).
11. The plaque-rich GSS cases include several different PrP mutations and variable transmissibility [P. Brown, *Rev. Neurol*. **148**, 317 (1992); B. Ghetti *et al*., *Sem. Virol*. **7**, 189 (1996) and reviewed in (*5*)].
12. G. Telling *et al*., *Science* **274**, 2079 (1996). The congophilic plaques described in P1 mice and rats from this progenitor strain were associated with the inoculation site and adjacent subependyma and white matter but were not reproduced on serial passage [J. Tateishi, H. Nagara, K. Hikita, Y. Sato, *Ann. Neurol.* **15**, 278 (1984)].
13. These people also lack any of the other relatively infrequent PrP mutations thought to enhance susceptibility to CJD or GSS, although they do have an unrelated Met^{129} homozygosity, a polymorphism present in 38% of the human population.
14. P. Brown, in *Immunologic Mechanisms in Neurologic and Psychiatric Disease*, B. Waksman, Ed. (Raven, New York, 1990), pp. 305–313; S. Prusiner, *Sci. Am.* **272**, 30 (January 1995).
15. L. Manuelidis and W. Fritch, *Virology* **215**, 46 (1996). The fastest strain will preferentially survive during the >15-year passage. Because the determined doubling time is 7.5 days, each year of continuous passage (two or more per year) represents ~248 doublings. Additionally, cross-species transmission can mimic strain selection by limiting dilution (*7*), because P1 incubation times and "takes" correspond to about one infectious dose.
16. Sprague-Dawley rats were inoculated intracerebrally with 50 μl of a 10% SY–infected hamster brain. For serial passage, a slice of rat frontal cortex was homogenized. Five-micrometer deparafinized sections were used for antibody binding with standard alkaline phosphatase or peroxidase detectors. Primary antibodies were diluted >1:1000, except HLA-DR, which was diluted 1:300. Because standard methods for histological detection of PrP-res (hydrolytic autoclaving, formic acid treatment, and proteinase K digestion) produced artifactual vacuoles, we developed other pretreatments. Autoclaving 5-m paraffin sections for 12 min in 0.2 M citrate (pH 6.0) preserved neuropil structure, gave little PrP background in controls, and did not alter the staining pattern of other antibodies in double detections. For double labeling, polyclonal antibody P8-1 (against gel-purified PrP-res) was first detected with peroxidase development (~5 min) with alakaline phosphatase for the second mononclonal antibody (~5 min). Reversed detection showed the same pattern of labeling.
17. Normally, microglia are found around vessels but rarely within the grey parenchyma, and we used a KS antibody to delineate activated microglia. In accord with Fig. 1B, KS antibody to released chondroitin sulfate (clone 5D4; ICN Costa Mesa, CA) can stain a few "ramified" microglia in the normal rat cortex [A. Bertolotto *et al.*, *J. Histochem. Cytochem.* **41**, 481 (1993)]. The numerous reactive microglia in infected rats were enlarged and had many processes, making them morphologically comparable to activated HLA-DR (class II) microglia in Alzheimer's disease (*25*). Additionally, invariant chains (associated with major histocompatibility class II molecules in antigen presentation) are modified by chondroitin sulfate [M. F. Naujokas *et al.*, *Cell* **74**, 245 (1993)]. It has not yet been determined whether the increase in activated microglia shown here represents migrating or proliferating populations; the association of many KS microglia with thin-walled vessels in later passages could suggest entry (macrophage derivatives) from the bloodstream. Some KS-positive cells may be phagocytic as PrP-res increased in the cytoplasm at later passages, but these cells were negative for the macrophage marker ED-1.
18. L. Manuelidis, D. M. Tesin, T. Sklaviadis, E. E. Manuelidis, *Proc. Natl. Acad. Sci. U.S.A.* **84**, 5937 (1987).
19. E. E. Manuelidis, J. Kim, J. Angelo, L. Manuelidis, *ibid.* **73**, 223 (1976).
20. At early stages of clinical disease (~307 days), rats could not right themselves when hung on a cage grid upside down. About a week later, a footprint test documented tight circling and wobbling, whereas older control rats ran straight off the filter paper. As in P1 and P2, terminal rats were hunched and thin, with ruffled fur.
21. H. M. Wisniewski, M. E. Bruce, H. Fraser, *Science* **190**, 1108 (1975). Rat plaques with "very faint" Congo Red birefringence [E. Field, C. Raine, G. Joyce, *Acta Neuropathol.* **8**, 47 (1967)] and in three aged Sprague-Dawley rats [D. Vaughan and A. Peters, *J. Neuropath. Exp. Neurol.* **40**, (1981)] have not been reproducible. Moreover, many other scrapie isolates propagated in rats (*7*) [R. Kimberlin, S. Cole, C. Walker, *J. Gen. Virol.* **68**, 1875 (1987)] have shown only short incubation times (<200 days) and vacuolar change. In contrast, the plaques here developed only after serial propagation and were widespread and unrelated to the inoculation site.
22. H. Gomi *et al*., *Neurosci. Lett.* **166**, 171 (1994); R. Riek *et al*., *Nature* **382**, 180 (1996). Alignment of GenBank sequences also shows only a single Ile-to-Leu difference in rat versus mice at codon 139.
23. For time course experiments, two random rats were killed and the uninoculated halves of the brains were fixed in formalin (*16*). Submitted images and controls for ubiquitin, ApoJ, APLP, and ApoE will be reported in detail elsewhere (*27*). The other halves were used for blots. A small slice of unfixed cerebellum and cortex from each brain was pooled and homogenized in saline for studies of PrP on blots, whereas the remaining unfixed half-brains were used for isolation of RNA and Northern (RNA) blotting as described (*18*). Proteinase K production of PrP-res was optimized for yield and maximum detection sensitivity by quantitative chemiluminesce (*15*). With polyclonal P8-1 diluted 1:2400, longer exposures made 1 in 20,000 PrP molecules visually obvious whereas 16-bit digitization with standards indicated a detection sensitivity approaching 5 logs. Use of other antibodies to PrP peptides gave the same pattern of PrP-res accumulation.
24. The slightly lesser value for KS microglia as compared with that for vacuoles at 150 days is due to our exclusion of vacuolated cerebellum in scoring, because the internal granule layer normally contains some KS+ cells.
25. P. McGeer, S. Akiyama, S. Itagaki, E. McGeer, *Can. J. Neurol. Sci.* **16**, 516 (1989); P. McGeer, K. Kawamata, D. Walker, *Brain Res.* **579**, 337 (1992).
26. H. Slunt *et al*., *J. Biol. Chem.* **269**, 2637 (1994); B. Crain *et al*., *Am. J. Pathol.* **149**, 1087 (1996).
27. L. Manuelidis, in preparation.
28. J. Collinge, K. Sidle, J. Meads, J. Ironside, A. Hill, *Nature* **383**, 685 (1996).
29. L. Manuelidis, T. Sklaviadis, E. E. Manuelidis, *EMBO J.* **6**, 341 (1987).
30. C. I. Lasmézas *et al*., *Science* **275**, 402 (1997).
31. A. Akowitz, T. Sklaviadis, E. E. Manuelidis, L. Manuelidis, *Microb. Pathog*. **9**, 33 (1990); T. Sklaviadis, R. Dreyer, L. Manuelidis, *Virus Res.* **26**, 241 (1992); T. Sklaviadis, A. Akowitz, E. E. Manuelidis, L. Manuelidis, *Arch. Virol*. **112**, 215 (1990); M. Ozel, E. Baldauf, M. Beekes, H. Diringer, in *Transmisssible Subacute Spongiform Encephalopathies: Prion Diseases*, L. Court and B. Dodet, Eds. (Elsevier, Paris, 1996), pp. 369–373.
32. L. Manuelidis, T. Sklaviadis, A. Akowitz, W. Fritch, *Proc. Natl. Acad. Sci. U.S.A.* **92**, 5124 (1995).
33. M. Dron and L. Manuelidis, *J. Neurovirol.* **2**, 240 (1996).
34. K. K. Hsiao *et al*., *Ann. N.Y. Acad. Sci.* **724**, 241 (1994); L. Manuelidis, *ibid.*, p. 259; R. I. Carp *et al*., *Trends Neurosci.* **17**, 148 (1994); R. E. Race *et al*., *Neuron* **15**, 1183 (1995).
35. F. Tagliavini *et al*., in *Transmisssible Subacute Spongiform Encephalopathies: Prion Diseases*, L. Court and B. Dodet, Eds. (Elsevier, Paris, 1996), pp. 323–327; D. R. Brown, B. Schmidt, H. A. Kretzschmar, *Nature* **380**, 345 (1996).
36. H. Büeler *et al*., *Cell* **73**, 1339 (1993); S. Sakaguchi *et al*., *J. Virol.* **69**, 7586 (1995).
37. H. Diringer and B. Ehlers, *J. Gen. Virol.* **72**, 457 (1991).
38. E. E. Manuelidis, E. J. Gorgacz, L. Manuelidis, *Science* **200**, 1069 (1978); E. E. Manuelidis, J. H. Kim, J. R. Mericangas, L. Manuelidis, *Lancet* **ii**, 896 (1985); J. Tateishi, *ibid.*, p. 1074; H. Diringer, *Arch. Virol.* **82**, 105 (1984).
39. S. Betmouni, V. Perry, J. Gordon, *Neuroscience* **74**, 1 (1996); C. I. Lasmézas *et al*., in *Transmisssible Subacute Spongiform Encephalopathies: Prion Diseases*, L. Court and B. Dodet, Eds. (Elsevier, Paris, 1996), pp. 151–157; G. Outram, in *Slow Virus Diseases of Animals and Man*, R. Kimberlin, Ed. (North-Holland, Amsterdam, 1976); R. Kimberlin and P. Cunnington, *Microbiol. Lett.* **3**, 169- (1978); A. Fauci, *Nature* **384**, 529 (1996).

40. We thank I. Shvayetsky, Z. Y. Lu for technical assistance, and I. Alafuzoff for suggesting citrate autoclaving. The human GSS and BSE blocks were generously provided by J. Tateishi and J. Ironside, respectively. Supported by NIH grants NS12674 and NS34569.

30 January 1997; accepted 12 May 1997